Purinergic Signalling (2018) 14:345–357
https://doi.org/10.1007/s11302-018-9616-5

ORIGINAL ARTICLE

Involvement of $P2Y_{12}$ receptor of stellate ganglion in diabetic cardiovascular autonomic neuropathy

Jingjing Guo[1] · Xuan Sheng[1] · Yu Dan[1] · Yurong Xu[1] · Yuanruohan Zhang[2] · Huihong Ji[3] · Jiayue Wang[3] · Zixi Xu[3] · Hongyu Che[2] · Guodong Li[1,4] · Shangdong Liang[1] · Guilin Li[1]

Received: 28 December 2017 / Accepted: 26 June 2018 / Published online: 6 August 2018

Abstract

Diabetes as a chronic epidemic disease with obvious symptom of hyperglycemia is seriously affecting human health globally due to the diverse diabetic complications. Diabetic cardiovascular autonomic neuropathy (DCAN) is a common complication of both type 1 and type 2 diabetes and incurs high morbidity and mortality. However, the underlying mechanism for DCAN is unclear. It is well known that purinergic signaling is involved in the regulation of cardiovascular function. In this study, we examined whether the $P2Y_{12}$ receptor could mediate DCAN-induced sympathetic reflexes. Our results revealed that the abnormal changes of blood pressure, heart rate, heart rate variability, and sympathetic nerve discharge were improved in diabetic rats treated with $P2Y_{12}$ short hairpin RNA (shRNA). Meanwhile, the expression of $P2Y_{12}$ receptor, interleukin-1β (IL-1β), tumor necrosis factor-α (TNF-α), and connexin 43 (Cx43) in stellate ganglia (SG) was decreased in $P2Y_{12}$ shRNA-treated diabetic rats. In addition, knocking down the $P2Y_{12}$ receptor also inhibited the activation of p38 MARK in the SG of diabetic rats. Taken together, these findings demonstrated that $P2Y_{12}$ receptor in the SG may participate in developing diabetic autonomic neuropathy, suggesting that the $P2Y_{12}$ receptor could be a potential therapeutic target for the treatment of DCAN.

Keywords $P2Y_{12}$ receptor · Diabetic cardiovascular autonomic neuropathy · Stellate ganglia · Satellite glial cells

Introduction

Diabetes mellitus is mainly due to the defects of insulin secretion and/or insulin action, displaying chronic hyperglycemia accompanied by the disorders in carbohydrate, lipid, and protein metabolism [1]. The incidence of diabetes is fast increasing [2] and the number of patients with diabetes mellitus will rise from 415 million in 2015 to 642 million by 2040, according to the latest data from the International Diabetes Federation [3]. Diabetic cardiovascular autonomic neuropathy (DCAN) is one of the most common complications in diabetic patients [4]. DCAN is defined as the impairment of autonomic control of the cardiovascular system in the case of diabetes after exclusion of other causes [5]. The clinical manifestations of DCAN include sinus tachycardia, exercise intolerance, and orthostatic hypotension. DCAN is a risk marker of mortality and cardiovascular morbidity, and a promoter for diabetic nephropathy [6]. In addition, the prevalence of DCAN is increasing with age (up to 44% of patients with type 2 diabetes over 65) and diabetes duration (up to 65% in long-term type 2 diabetes) [4, 7]. The large number of patients with DCAN and the rather complex pathogenesis of DCAN cry for an urgent need to elaborate the underlying mechanism.

Adenosine triphosphate (ATP) and its analogues bind to P2 receptors [8–10]. P2 receptors can be divided into P2X and P2Y subgroups. Seven P2X ($P2X_{1-7}$) and eight P2Y ($P2Y_{1,2,4,6,11,12,13,14}$) receptor subtypes have been cloned in mammals [10]. The $P2Y_{12}$ receptor is a Gi-coupled ADP receptor, which is first described in blood platelets where it plays a central role in their activation and aggregation [11, 12]. The $P2Y_{12}$ receptor participates in arterial thrombosis and is an established target of antithrombotic drugs like the

✉ Guilin Li
liguilin@ncu.edu.cn

1 Department of Physiology, Medical College of Nanchang University, Nanchang 330006, China

2 Queen Mary School, Medical College of Nanchang University, Nanchang 330006, China

3 Department of the First Clinical, Medical College of Nanchang University, Nanchang 330006, China

4 Department of Anatomy, Yong Loo Lin School of Medicine, National University of Singapore, Singapore, Singapore

thienopyridine compounds (e.g., ticlopidine, clopidogrel, and prasugrel) or the direct, reversible antagonists such as ticagrelor and cangrelor [12]. Recent studies have revealed that the $P2Y_{12}$ receptor is also expressed in both the microglia of the central nervous system and satellite glial cells of the peripheral ganglia [13–16], suggesting that it may play a key role in microglial activation especially in the early stages [14].

Purinergic signaling may also participate in the regulation of cardiovascular function [17]. Studies showed that the $P2Y_{12}$ receptor antagonist ticagrelor could enhance adenosine-induced coronary vasodilatory responses in humans [18, 19]. $P2Y_{12}$ inhibitors could lead to significant attenuation of injury of myocardium in diabetic animals [20] and resulted in a significant reduction in infarct size when administered prior to the onset of reperfusion [21]. Moreover, the $P2Y_{12}$ receptor in the dorsal root ganglia might be involved in diabetic neuropathic pain [22]. Thus, $P2Y_{12}$ receptor may play an important role in developing diabetic cardiovascular complications.

The autonomic ganglia include sympathetic and parasympathetic ones. The cervical sympathetic nervous system contributes to the maintenance of cardiovascular homeostasis [23]. Cardiac sympathetic innervation is largely made by the superior cervical ganglia (SCG) and the stellate ganglia (SG) [24]. The latter distributes to the cardiac plexus, receiving and integrating the afferent and efferent signals and thus regulating heart function [25]. Stellate ganglion block is widely used in the treatment of heart diseases [26]. Stellate ganglion neurons are often surrounded by satellite glial cells (SGCs) [27]. Axotomy, inflammation, and other injuries can activate the SGCs of primary sensory ganglia [28]. $P2Y_{12}$ receptor is expressed in SGCs [23, 29–31] and may participate in bidirectional neuronal-glial communications [15, 32]. However, little is known whether $P2Y_{12}$ receptor is implicated in DCAN. The purpose of this study was to explore the potential role of $P2Y_{12}$ receptor in DCAN and underlying mechanisms.

Materials and methods

Animal models and groups

Adult male Sprague-Dawley rats (200–250 g) were provided by the Center of Laboratory Animal Science of Nanchang University. The use of animals was reviewed and approved by the Animal Care and Use Committees of Nanchang University Medical Schools. All rats were housed in standard metabolic cages (three rats each) and kept at 40–70% humidity and room temperature (21–25 °C). Control rats (Ctrl, $n = 10$) were free to obtain water and common diet (which consisted of 53% carbohydrate, 23% protein, and 5% fat). Type 2 diabetic model rats were given a high-fat and high-sugar diet (66.5% basal diet, 20% sugar, 10% oil, 2.5% cholesterol, and 1% sodium cholate) for 4 weeks. Subsequently, diabetic model rats were injected intraperitoneally with a low dose of streptozotocin (STZ, 30 mg/kg) [33]. After 1 week of STZ injection, blood glucose was measured. Diabetic rats were defined as fasting plasma glucose (FPG) ≥ 7.8 mM or postprandial blood glucose (PBG) ≥ 11.1 mM [33–35]. Diabetic rats were continuously fed with high-fat and high-sugar diet for additional 2 weeks after verified as hyperglycemic.

To test the effects of $P2Y_{12}$ short hairpin RNA (shRNA), type 2 diabetic rats were randomly divided into three groups ($n = 10$ in each group): type 2 diabetic group (DM), type 2 diabetic rats treated with $P2Y_{12}$ shRNA group (DM+$P2Y_{12}$ shRNA) and type 2 diabetic rats treated with scramble shRNA negative control group (DM+NC shRNA). The $P2Y_{12}$ shRNA and scramble shRNA were constructed by Novobio Company of Shanghai. The Entranster™ - in vivo transfection reagents were provided by Engreen Company of Beijing. According to the manufacturer's instructions, a mixture of 10 μg $P2Y_{12}$ shRNA and 20 μl transfection reagent was injected into the sublingual vein for the DM+$P2Y_{12}$ shRNA group. And for the DM+NC shRNA group, a mixture of 10 μg scramble shRNA and 20 μl transfection reagent was injected. The same volume of saline was injected into the control and DM group. After 1 week, the rats were anesthetized with intraperitoneal administration of 50 mg/kg sodium pentobarbital, and the SGs were collected.

To assess the effect of $P2Y_{12}$ overexpression, rats were randomly divided into three groups: control group (Ctrl with no injections), control rats treated with pcDNA3.1- $P2Y_{12}$ plasmid group (Ctrl+$P2Y_{12}$), and control rats treated with pcDNA3.1 empty vector as negative control group (Ctrl+vector). The pcDNA3.1-$P2Y_{12}$ plasmid or pcDNA3.1 plasmid vector was injected into left stellate ganglia at a dose of 5 μg/20 μL per rat via Entranster™ - in vivo transfection reagents [36]. After 4 days, blood pressure, heart rate, and sympathetic nerve discharge were measured.

Measurements of blood pressure, heart rate, and sympathetic nerve activity

Blood pressure and heart rate were measured using an indirect tail-cuff method (Softron BP-98 A, Softron Co., Tokyo, Japan). Heart rate variability (HRV) was analyzed using electrocardiogram (ECG) recording by the frequency domain. The power of the RR-interval variations in the whole frequency range of the spectrum (total power frequency, TP, 0–0.5 Hz) and in the range of very-low frequency (VLF, 0.003–0.04 Hz), low frequency (LF, 0.04–0.15 Hz), and high frequency (HF, 0.15–0.40 Hz) were calculated from short-term recordings of 5 min. LF indicates sympathetic activity and HF indicates parasympathetic activity.

The postganglionic cervical sympathetic nerve discharge (SND) of SG was recorded and analyzed using a RM6240 biological signal analytical system (Chengdu Instrument Factory, Chengdu, China). In brief, four groups of rats were anesthetized with pentobarbital sodium (50 mg/kg, i.p.). The left cervical sympathetic nerve was identified and immersed in warm paraffin. Silver electrodes connected to the RM6240 system for recording SND were attached to the cervical sympathetic nerve, and the reference electrode to a skin fold. The settings for the SND patterns were as follows: recording sensitivity (25–50 μV), scanning speed (200 ms/div), power gain (200 μV), time constant (0.001 s), and frequency filtering (3 kHz). Cervical SND was integrated and quantified as μvolts × seconds (μV s) [37, 38].

Quantitative real-time PCR

Total RNA was isolated from the SG using the TRIzol Total RNA Reagent (Beijing Tiangen Biotech Co.). The reverse transcription reaction was completed using a RevertAid™ First Strand cDNA Synthesis Kit (Fermentas, Glen Bernie, MD, USA) following the manufacturer's instructions. The primers were designed with the Primer Express 3.0 software (Applied Biosystems, Inc., Foster City, CA, USA), and the sequences were as follows: sense GCTCTCTTCCAGCC TTCCTT and anti-sense CTTCTGCATCCTGTCAGCAA for β-actin; sense CTTCGTTCCCTTCCACTTTG and anti-sense AGGGTGCTCTCCTTCACGTA for $P2Y_{12}$; sense CCTATGTCTTGCCCGTGGAG and anti-sense CACACACTAGCAGGTCGTCA for interleukin-1β (IL-1β); sense ATGGGCTCCCTCTCATCAGT and anti-sense GCTTGGTGGTTTGCTACGAC for tumor necrosis factor-α (TNF-α); sense GGTGTCCTTGGTGTCTCTCG and anti-sense CTTCACGCGATCCTTAACGC for Cx43. Quantitative PCR was performed using SYBR® Green Master Mix on an ABI PRISM® 7500 Sequence Detection System (Applied Biosystems, Inc., Foster City, CA, USA). The quantification of gene expression was calculated by the $2^{-\Delta\Delta Ct}$ method in comparison with respective levels of β-actin mRNA.

Western blotting

Total protein was extracted by homogenizing the SG samples by mechanical disruption in lysis buffer (50 mM Tris–Cl, pH 8.0, 150 mM NaCl, 0.1% sodium dodecyl sulfate (SDS), 1% Nonidet P-40, 0.02% sodium deoxycholate, 100 μg/ml phenylmethylsulfonyl fluoride, 1 μg/ml aprofinin, 1% phosphatase inhibitors, and 1% protease inhibitors) and incubating on ice for 40 min. The lysates were centrifuged at 12,000×*g* for 15 min at 4 °C. The supernatants were collected to measure protein concentrations using a bicinchoninic acid assay reagent kit and then stored at − 20 °C until use. Upon Western blotting, the supernatants were diluted with sample buffer (250 mM Tris–Cl, 200 mM dithiothreitol, 10% SDS, 0.5% bromophenol blue, and 50% glycerol) and denatured by heating at 95 °C for 5 min. Supernatant samples containing 20 μg protein were loaded onto 10% SDS-polyacrylamide gels for electrophoresis and then transferred to polyvinylidene fluoride (PVDF) membranes. The PVDF membranes were blocked for 1 h at room temperature in 5% nonfat dried milk in 25 mM Tris-buffered saline (pH 7.2) plus 0.05% Tween-20 (TBST). The membranes were incubated with the primary rabbit antibodies against $P2Y_{12}$ (1:1000, Cat# ab184411; Abcam, Cambridge, UK), IL-1β (1:500, AF5103; Affinity, Golden, CO, USA), TNF-α (1:500, AF7014; Affinity, Golden, CO, USA), p38 mitogen-activated protein kinases (p38 MAPK) (1:1000, 8690; Cell Signaling Technology, Danvers, MA, USA), phosphorylated p38 MAPK (p-p38 MAPK) (1:1000, 4511; Cell Signaling Technology, Danvers, MA, USA), mouse anti-connexin 43 (Cx43) (1:1000, ab79010; Abcam, Cambridge, UK), or mouse anti-glutamine synthetase (GS) (1:1500, ab64613; Abcam, Cambridge, UK) for overnight at 4 °C. After three washes with TBST, the membranes were incubated with one of horseradish peroxidase-conjugated secondary antibodies: goat anti-rabbit IgG or goat anti-mouse IgG (1:2000, Beijing Zhongshan Biotechnology Co.) for 1 h at room temperature. Protein signal was visualized and detected using a chemiluminescence gel imaging system (XRS+, Bio-Rad Company, USA). The membranes were stripped and incubated with mouse anti-β-actin (1:2000, A3854; Sigma-Aldrich, St. Louis, MO, USA) to verify equally loading the samples. The changes of integrated optical density (IOD) for the protein of interest were analyzed with Image Pro-Plus software.

Immunohistochemistry

Collected SGs were washed in phosphate-buffered saline (PBS), and then fixed in 4% paraformaldehyde (PFA) for 24 h at 4 °C. The specimen was transferred to 20% sucrose in 4% PFA and kept overnight. Tissues were sectioned at a thickness of 8 μm with a freezing microtome. The sections were mounted onto the glass slides and then stored at − 20 °C for further processing. Co-expression of $P2Y_{12}$ and GS or calcitonin gene-related peptide (CGRP) and co-localization of p-p38 MARK with CGRP were observed by double-label immunofluorescence staining. The sections were washed with PBS and punched with 0.3% Triton X-100 for 10 min at room temperature. Following 30-min incubation with blocking solution, the sections were incubated with mouse anti-GS (1:150, Cat# ab64613; Abcam, Cambridge, UK) and rabbit anti-$P2Y_{12}$ (1:150, ab184411; Abcam, Cambridge, UK) overnight at 4 °C. The sections were then rinsed and incubated with TRITC (tetraethyl rhodamine isothiocyanate)-labeled goat anti-rabbit IgG (1:150, Beijing Zhongshan Biotech

CO.) or FITC (fluorescein isothiocyanate)-labeled goat anti-mouse IgG (1:150, Beijing Zhongshan Biotech Co.) for 1 h at 37 °C. For coexpression of $P2Y_{12}$ and CGRP, the sections were incubated with mouse anti-CGRP (1:150, ab81887; Abcam, Cambridge, UK) and rabbit anti-$P2Y_{12}$ (1:150) overnight at 4 °C, followed by rinsing and incubating sections with TRITC-labeled goat anti-mouse IgG or FITC-labeled goat anti-rabbit IgG for 1 h at 37 °C. For colocalization of p-p38 MARK with CGRP, the sections were incubated with mouse anti-CGRP (1:150) and rabbit anti-p-p38 MARK (1:150, 4511; Cell Signaling Technology, Danvers, MA, USA) overnight at 4 °C, and further processed using fluorescent probe-labeled secondary antibodies in the same way as described above. The completed sections were rinsed and mounted with anti-fluorescent quenching agent. For detecting the expression of Cx43, sections were processed in 3% H_2O_2, blocked by normal goat serum, and incubated with the primary antibody mouse anti-Cx43 (1:150, ab79010; Abcam, Cambridge, UK) for overnight at 4 °C, followed by incubating with biotinylated secondary antibody (1:200; Beijing Zhongshan Biotech Co.) and processing with DAB (Beijing Zhongshan Biotech Co.). All images were captured by fluorescence microscopy (Olympus DP72, Japan) under the same exposure, light, hue, and contrast conditions. The yellow fluorescence density (coexpression level) of each image was analyzed by Image-Pro Plus software. Immunofluorescence intensity was measured in a square region of interest (100 × 100 μm). The mean optical density value from each region of interest was normalized against the background defined as the signal measured in an area devoid of specific immunostaining. Data were collected from five discontinuous slices of each rat with six rats in each group.

Statistical analysis

Statistical analysis of the data was performed on SPSS 11.5 software. All results were expressed as mean ± SEM. Cervical SND responses were reported as both percentage change from baseline values (control) and in absolute terms (μV s). Control values of cervical SND were considered as 100%. Significant differences were evaluated using one-way ANOVA followed by Dunnett's or Tukey's tests. $p < 0.05$ was considered to have a significant difference.

Results

Elevated expression of $P2Y_{12}$ receptor in the SG of DM rats was inhibited by $P2Y_{12}$ shRNA

Real-time PCR results (Fig. 1a) showed that the expression levels of $P2Y_{12}$ receptor in DM group were significantly higher than those in control group ($p < 0.01$). The mRNA levels of $P2Y_{12}$ receptor in DM+$P2Y_{12}$ shRNA group were decreased compared to that in DM group ($p < 0.01$). There was no significant difference between DM group and DM+NC shRNA group, nor between control group and DM+$P2Y_{12}$ shRNA group ($p > 0.05$).

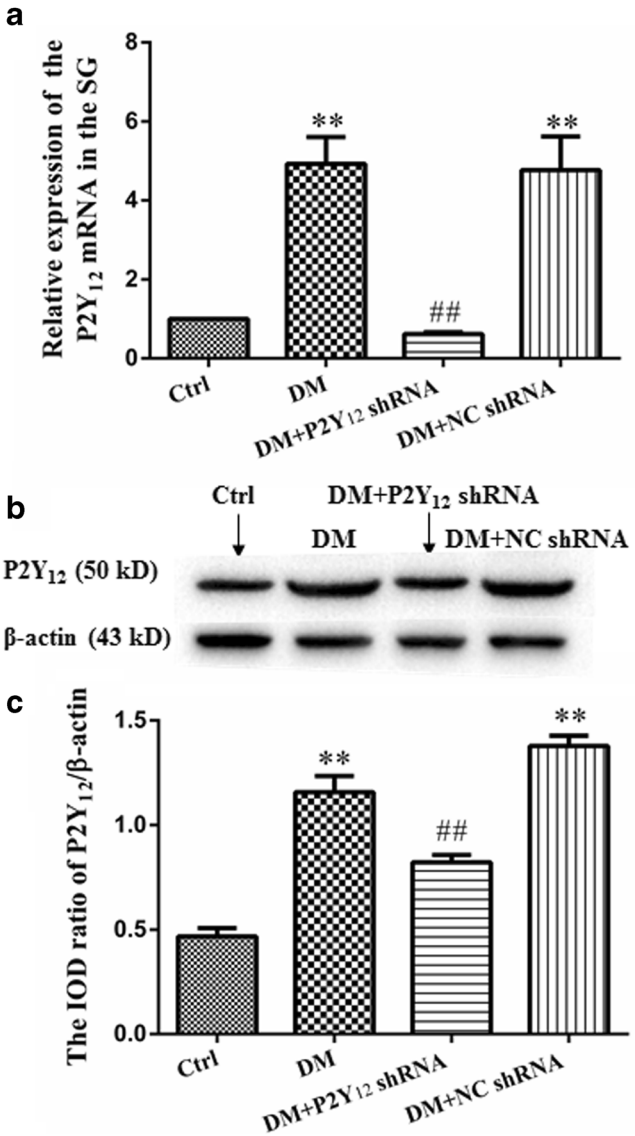

Fig. 1 The expression levels of $P2Y_{12}$ receptor mRNA and protein in SG of type 2 diabetic rats. **a** The expression of $P2Y_{12}$ mRNA was detected by real-time PCR analysis using β-actin as internal control. Values are mean ± SEM of fold changes from three independent experiments. **b** The protein level of $P2Y_{12}$ was measured by Western blotting. **c** The bar histograms show the integrated optical density (IOD) ratio of $P2Y_{12}$ protein level to β-actin in each group and the values are mean ± SEM from three independent experiments. $^{**}p < 0.01$ vs. Ctrl; $^{\#\#}p < 0.01$ vs. DM

The expression of $P2Y_{12}$ was further analyzed at protein level by Western blotting (Fig. 1b). By image analysis, the stain values (integrated optical density, IOD) of $P2Y_{12}$ protein mass (normalized to individual β-actin internal control) in DM group were significantly higher than that in control group ($p < 0.01$). In addition, the IOD of $P2Y_{12}$ in DM+$P2Y_{12}$ shRNA group

Table 1 Effects of $P2Y_{12}$ shRNA on heart rate and blood pressure in rats

Group	Heart rate (beat/min)	Blood pressure		
		SBP (mm Hg)	DBP (mm Hg)	MBP (mm Hg)
Ctrl	317.2 ± 12.04	106.71 ± 13.56	80.21 ± 8.68	87.61 ± 8.96
DM	363.97 ± 39.87**	129.96 ± 11.89**	85.74 ± 9.58**	96.49 ± 9.37**
DM+$P2Y_{12}$ shRNA	318.28 ± 11.9$^{\#\#}$	112.48 ± 6.46$^{\#\#}$	76.48 ± 11.95$^{\#\#}$	88.6 ± 7.89 $^{\#\#}$
DM+NC shRNA	354.56 ± 27.83**	130.25 ± 12.99**	86.44 ± 9.16**	98.75 ± 10.97**

Values are mean ± SEM from ten observations in each group

SBP systolic blood pressure, *DBP* diastolic blood pressure, *MBP* mean arterial pressure

**$p < 0.01$ vs. Ctrl; $^{\#\#}p < 0.01$ vs. DM

was reduced compared with DM group ($p < 0.01$). No significant difference was seen between DM group and DM+NC shRNA group, nor between Ctrl and DM+$P2Y_{12}$ shRNA group ($p > 0.05$; Fig. 1c). These results indicated that $P2Y_{12}$ shRNA treatment may counteract the upregulated expression of $P2Y_{12}$ in SGs of diabetic rats.

Targeting $P2Y_{12}$ by shRNA improved the abnormal changes of heart rate, blood pressure, and sympathetic nerve activity in DM rats

The heart rate (HR), systolic blood pressure (SBP), diastolic blood pressure (DBP), and mean arterial pressure (MBP) were increased in the DM group compared to that in the control group ($p < 0.01$). By contrast, the upregulated SBP, DBP, MBP, and HR were diminished in DM treated with $P2Y_{12}$ shRNA ($p < 0.01$; Table 1). There was no significant difference in these cardiovascular parameters between DM+NC shRNA group and DM group, and nor between control and DM+$P2Y_{12}$ shRNA group ($p > 0.05$).

The postganglionic cervical SND of SG in the DM group was significantly enhanced compared with that in the control group ($p < 0.01$). After treatment of DM rats with $P2Y_{12}$ shRNA, the cervical SND was significantly decreased compared with that in the untreated DM group ($p < 0.01$). No significant difference was observed between DM+NC shRNA group and DM group, nor between control and DM+$P2Y_{12}$ shRNA group ($p > 0.05$; Fig. 2). The elevated blood pressure, increased heart rate, and sympathetic nerve activity in DM rats suggested an increase of excitability in cardiac sympathetic nerve.

Overexpression of $P2Y_{12}$ increased heart rate, blood pressure, and sympathetic nerve activity in control rats

The HR, SBP, DBP, and MBP were increased in the Ctrl+$P2Y_{12}$ group compared to that in the control group. There was no significant difference in these cardiovascular parameters between Ctrl group and Ctrl+vector group ($p > 0.05$; Table 2).

The postganglionic cervical SND of SG in the Ctrl+$P2Y_{12}$ group was significantly enhanced compared with that in the control group ($p < 0.01$). No significant difference was observed between Ctrl group and Ctrl+vector group ($p > 0.05$; Fig. 3). The elevated blood pressure, increased heart rate, and

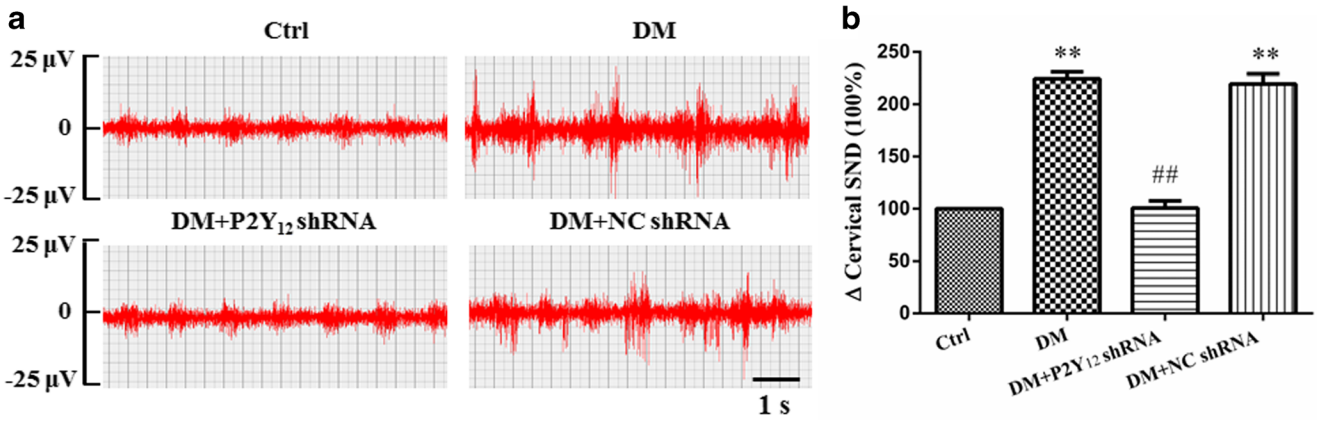

Fig. 2 The effects of $P2Y_{12}$ shRNA on the cervical sympathetic nerve activity of type 2 diabetic rats. **a** Representative images of the postganglionic cervical sympathetic nerve discharge of SG. **b** Integrated cervical sympathetic discharge in all groups. Data are represented as means ± SEM ($n = 8$). **$p < 0.01$ vs. Ctrl; $^{\#\#}p < 0.01$ vs. DM

Table 2 Effects of $P2Y_{12}$ overexpression on heart rate and blood pressure in rats

Group	Heart rate (beat/min)	Blood pressure		
		SBP (mm Hg)	DBP (mm Hg)	MBP (mm Hg)
Ctrl	316.85 ± 13.11	105.88 ± 10.5	80.45 ± 6.45	86.99 ± 8.23
Ctrl+$P2Y_{12}$	351.43 ± 32.16*	125.59 ± 11.41**	85.09 ± 7.37	95.92 ± 8.45*
Ctrl+vector	317.92 ± 18.11	108.57 ± 10.9	81.91 ± 8.73	88.41 ± 8.28

Values are mean ± SEM from six observations in each group

*$p < 0.05$, **$p < 0.01$ vs. Ctrl

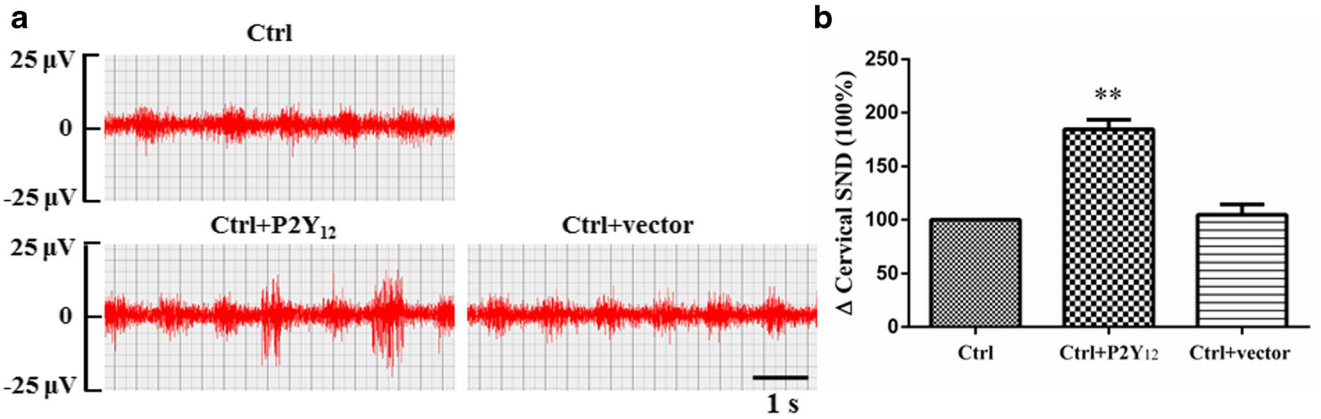

Fig. 3 The effects of overexpression of $P2Y_{12}$ on the cervical sympathetic nerve activity of control rats. **a** Representative images of the postganglionic cervical sympathetic nerve discharge of SG. **b** Integrated cervical sympathetic discharge in all groups. Data are represented as means ± SEM ($n = 6$). **$p < 0.01$ vs. Ctrl

sympathetic nerve activity in the $P2Y_{12}$ overexpressed rats suggested that the upregulated $P2Y_{12}$ receptor could increase the excitability in cardiac sympathetic nerve.

Targeting $P2Y_{12}$ by shRNA decreased LF/HF ratio of HRV in DM rats

The effects of shRNA targeting $P2Y_{12}$ on heart rate variability (HRV) are shown in Table 3. In DM and DM+NC shRNA group, the total power frequency (TP), very-low frequency (VLF), low frequency (LF), and high frequency (HF) were decreased compared with those in control group ($p < 0.01$), suggesting that both sympathetic and parasympathetic tones were reduced in DM. In addition, LF/HF ratio was significantly increased in DM, pointing to a stronger inhibition of parasympathetic activity than sympathetic activity, because LF reflected the former and HF reflected the latter. $P2Y_{12}$ shRNA treatment increased the TP, VLF, LF, and HF but decreased the LF/HF ratio in type 2 diabetic rats ($p < 0.01$), suggesting that $P2Y_{12}$ shRNA alleviated the relatively high sympathetic tone in DM rats. There was no significant difference between

Table 3 Effects of $P2Y_{12}$ shRNA on heart rate variability in rats

	TP (ms^2)	VLF (ms^2)	LF (ms^2)	HF (ms^2)	LF/HF
Ctrl	137.01 ± 14.34	119.3 ± 12.35	6.84 ± 0.78	11.97 ± 1.69	0.58 ± 0.05
DM	108.96 ± 11.54**	106.3 ± 11.09**	2.27 ± 0.29**	0.89 ± 0.09**	2.39 ± 0.34**
DM+$P2Y_{12}$ shRNA	135.56 ± 13.91##	123.02 ± 15.06##	5.18 ± 0.44##	10.12 ± 1.31##	0.52 ± 0.05##
DM+NC shRNA	108.36 ± 11.55**	104.19 ± 13.25**	2.71 ± 0.24**	1.29 ± 0.29**	1.97 ± 0.23**

Values are mean ± SEM from ten observations in each group

TP total power frequency, *VLF* very-low frequency, *LF* low frequency, *HF* high frequency

**$p < 0.01$ vs. Ctrl; ## $p < 0.01$ vs. DM

DM+NC shRNA and DM group, nor between control and DM+P2Y$_{12}$ shRNA group ($p > 0.05$).

Colocalization of P2Y$_{12}$ receptor and GS in SGCs of SG

Since upregulated expression of GS is a typical characteristic of SGC activation, the colocalization of the P2Y$_{12}$ receptor and GS (a marker of SGCs) was measured using double-label immunofluorescence staining (Fig. 4a). The coexpression levels of P2Y$_{12}$ and GS in the DM group were higher than those in the control group, whereas P2Y$_{12}$ shRNA treatment could antagonize such upregulated coexpression of P2Y$_{12}$ and GS ($p < 0.01$; Fig. 4b). Moreover, the intensity of staining of P2Y$_{12}$ in SG was changed in parallel to that of GS. In addition, Western blotting also indicated that the expression level of GS protein in the DM group was higher than that in the control group, whereas P2Y$_{12}$ shRNA treatment could antagonize such upregulated expression of GS

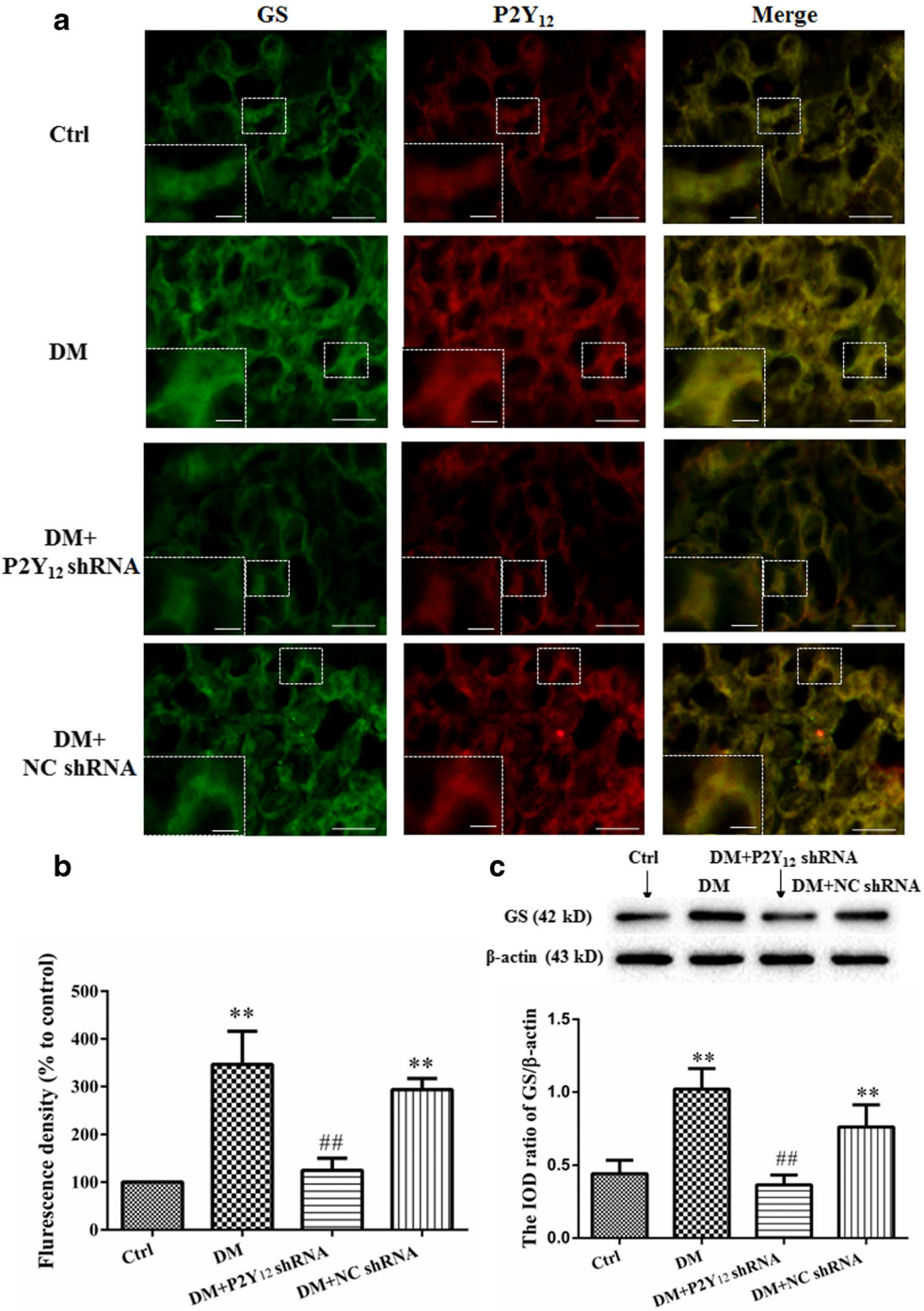

Fig. 4 The double-label immunofluorescence staining of P2Y$_{12}$ and GS and the expression of GS protein in SG. **a** Coexpression of P2Y$_{12}$ receptor and GS was seen in the SG. The green signal represents GS staining with FITC, and the red signal indicates P2Y$_{12}$ staining with TRITC. Merged image denotes the P2Y$_{12}$ and GS double staining. Scale bar, 20 μm; insets, 5 μm ($n = 6$ in each group). **b** Quantification of P2Y$_{12}$ receptor and GS immunostaining (yellow) fluorescence. The yellow fluorescence density in control group was considered as 100% ($n = 6$ in each group). **c** The protein level of GS was measured by Western blotting. The bar histograms show the IOD ratio of GS protein level to β-actin in each group, and the values are mean ± SEM from three independent experiments. $^{**}p < 0.01$ vs. Ctrl; $^{\#\#}p < 0.01$ vs. DM

($p < 0.01$; Fig. 4c). The pattern of such changes of GS expression in SG was also observed for $P2Y_{12}$ under similar experimental conditions (see Fig. 1b). These results indicated that $P2Y_{12}$ receptor was expressed in the SGCs of SG, and furthermore, upregulated coexpression of GS and $P2Y_{12}$ receptor occurred in the SGCs of SG under diabetic condition.

Double-label immunofluorescence staining detected expression of $P2Y_{12}$ receptor and CGRP in SG

We also detected $P2Y_{12}$ and CGRP in SG by double-label immunofluorescence staining (Fig. 5). The results showed that CGRP was expressed in neurons whereas $P2Y_{12}$ was surrounded rather than colocalized with the neuron, which also indicated that $P2Y_{12}$ receptor was expressed in SGCs rather than neurons.

Targeting $P2Y_{12}$ by shRNA reduced expression of IL-1β and TNF-α in SG

Activated SGCs can release many inflammatory factors. The results from real-time PCR showed that the expression levels of IL-1β and TNF-α were significantly increased in DM group compared with those in control group ($p < 0.01$). The levels of IL-1β and TNF-α mRNA in DM+$P2Y_{12}$ shRNA group were decreased compared with those in DM group ($p < 0.01$). There was no significant difference either between DM group and DM+NC shRNA group, or between control group and DM+$P2Y_{12}$ shRNA group ($p > 0.05$; Fig. 6a).

The expression of IL-1β and TNF-α was further examined at protein level by Western blotting (Fig. 6b). The results showed that IL-1β and TNF-α protein mass in DM group were significantly higher than that in control group ($p < 0.01$). In addition, treatment with $P2Y_{12}$ shRNA could diminish the IL-1β and TNF-α protein mass in DM group ($p < 0.01$). There was no significant difference between DM group and DM+NC shRNA group, nor between control and DM+$P2Y_{12}$ shRNA group ($p > 0.05$; Fig. 6c).

Targeting $P2Y_{12}$ by shRNA lowered expression of Cx43 in SG

Cx43 is an important and common gap-junction protein in the body and is associated with nerve damage. The immunohistochemistry staining results revealed that Cx43 was expressed in the SGCs of SG (Fig. 7a). Real-time PCR results showed that the expression of Cx43 in diabetic rats was increased compared with that in control rats ($p < 0.01$). The levels of Cx43 mRNA in DM+$P2Y_{12}$ shRNA group were lower than those in DM group ($p < 0.01$). There was no significant difference either between DM group and DM+NC shRNA group, or between control and DM+$P2Y_{12}$ shRNA group ($p > 0.05$; Fig. 7b). Western blotting analysis indicated that the protein mass of Cx43 was also increased in DM rats compared with control rats ($p < 0.01$; Fig. 7c). Treatment with $P2Y_{12}$ shRNA significantly relieved the upregulated Cx43 mass in DM rats ($p < 0.01$). There was no significant difference between DM group and DM+NC shRNA group, nor between control and DM+$P2Y_{12}$ shRNA group ($p > 0.05$; Fig. 7d).

Targeting $P2Y_{12}$ by shRNA mitigated phosphorylation of p38 MAPK in SG

The cellular localization of p-p38 MAPK and CGRP in SG was observed by double-label immunofluorescence staining (Fig. 8a). The results showed that p-p38 MAPK was colocalized with CGRP, which indicated that p-p38 MAPK was expressed in neurons of SG.

The expression levels of both p38 MAPK and p-p38 MAPK were assessed by Western blotting (Fig. 8b). There was no significantly difference among the four groups for the IOD ratio of p38 MAPK to β-actin ($F_{(3, 20)} = 0.89$, $p = 0.46$,data not shown). However, the IOD ratio of p-p38 MAPK to p38 MAPK in DM group was higher than that in the control group ($p < 0.01$). Compared with DM group, the IOD ratio of p-p38 MAPK to p38 MAPK in the DM+$P2Y_{12}$ shRNA group was decreased ($p < 0.01$). There was no significant difference either between DM group and DM+NC shRNA group, or between control and DM+$P2Y_{12}$ shRNA

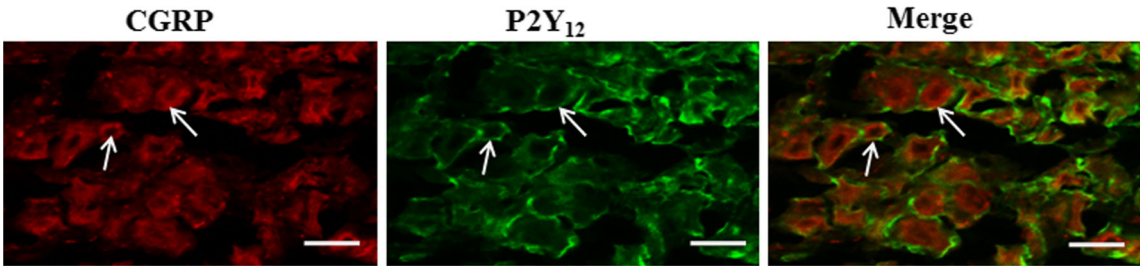

Fig. 5 The double-label immunofluorescence staining of $P2Y_{12}$ and CGRP in SG. The expression of $P2Y_{12}$ receptor and CGRP in SG was detected by double-label immunofluorescence staining. The green signal represents $P2Y_{12}$ staining with FITC, and the red signal indicates CGRP staining with TRITC. The merged image represents the double staining of $P2Y_{12}$ and CGRP. Scale bar, 20 μm

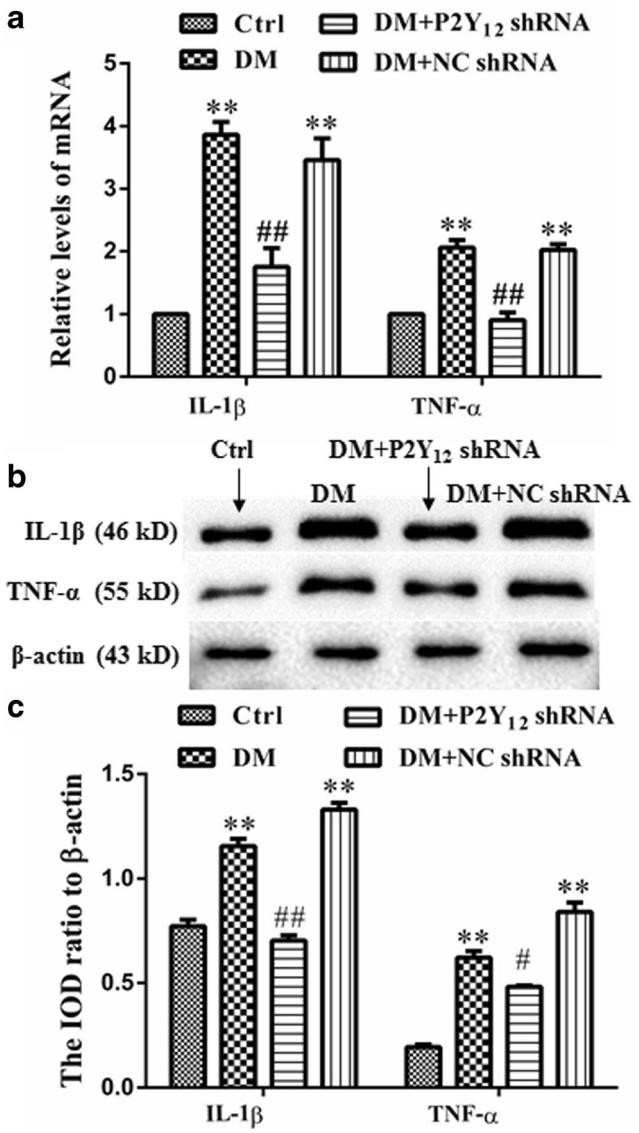

Fig. 6 The effects of $P2Y_{12}$ shRNA on expression levels of IL-1β and TNF-α mRNA and protein in SG of type 2 diabetic rats. **a** The expression levels of IL-1β and TNF-α mRNA were determined by real-time PCR analysis using β-actin as internal control. Results were expressed as mean ± SEM of fold changes from three independent experiments. **b** The protein levels of IL-1β and TNF-α were measured by Western blotting. **c** The bar histograms show the IOD ratio of IL-1β and TNF-α protein level to β-actin in each group. Values are mean ± SEM from three independent experiments. $^{**}p < 0.01$ vs. Ctrl; $^{\#}p < 0.05$, $^{\#\#}p < 0.01$ vs. DM

group ($p > 0.05$; Fig. 8c). These results indicated that the phosphorylation of p38 MAPK in SG was correlated with the enhanced $P2Y_{12}$ receptor-mediated sympatho-excitatory responses in DM rats.

Discussion

Subjects with diabetes frequently suffer from DCAN [39]. Upon injury and nociceptive stimulation, the damaged cells, stressed cells, and nerve endings release a large amount of ATP. Inflammatory substances such as ATP and its receptors (P2X and P2Y) are involved in the transmission of nociceptive information. ATP can modulate cardiac function [18, 40]. P2Y receptors are activated by purine, pyrimidine nucleotides or sugar-nucleotides, producing intracellular second-messengers through stimulating heterotrimeric G-proteins [10, 41]. The $P2Y_{12}$ receptor is expressed in human β-cells and brown adipocytes, in rodent pancreas (islet and cell preparations) and in β-cell lines, and may be involved in diabetes [42]. The cervical sympathetic ganglion neurons participate in regulating the function of heart and blood vessels [17]. The cardiovascular complications of diabetes involve the damage of autonomic nerve fibers that control heart and blood vessels, leading to abnormalities in heart rate control, vascular dynamics, and sympathetic nerve activity [43]. Upregulation of $P2Y_{12}$ signaling occurs in hyperglycemia, and $P2Y_{12}$ receptor inhibition reduces the adverse events following percutaneous coronary intervention [44]. Our data showed that the expression of $P2Y_{12}$ receptor in SG at both $P2Y_{12}$ mRNA and protein levels was increased in diabetic rats and $P2Y_{12}$ shRNA treatment could alleviate the elevated expression. Moreover, our results revealed that $P2Y_{12}$ shRNA reduced the elevated blood pressure, heart rate, and cervical SND induced by diabetes, whereas the overexpression of $P2Y_{12}$ receptor increased blood pressure, heart rate, and cervical SND in the control rats, indicating that $P2Y_{12}$ receptor may be actively involved in DCAN. Thus, it suggests that upregulation of $P2Y_{12}$ receptor may be relevant to the pathophysiological cardiovascular changes in diabetes.

The assessment of HRV has been a well-accepted method to evaluate the status of autonomic control of the heart. In diabetics, the reduction in HRV is attributed to the cardiac self-injury, which occurs early in hyperglycemic settings [45]. Loss of HRV was found to be an independent predictor of all-cause and cardiovascular mortality in population-based studies. Analysis of HRV in time and frequency domains reveals substantial information on the balance between sympathetic and parasympathetic innervation of the heart. In this study, TP, very-low frequency (VLF), LF and HF in type 2 diabetic rats were lower than those in control rats, indicating the impairing of both parasympathetic and sympathetic nerve activity. However, the increased ratio of LF/HF suggested that the parasympathetic nerve was more severely damaged. This would result in the imbalance between sympathetic and parasympathetic tones, and consequently, the sympathetic nerve was relatively more excited. After treatment with $P2Y_{12}$ shRNA in type 2 diabetic rats, the changes in TP, VLF, LF, HF, and the ratio of LF/HF were prevented. Thus, $P2Y_{12}$ receptor may play an important role in autonomic nerve injury in type 2 diabetes and downregulation of $P2Y_{12}$ receptor may be targeted to alleviate the autonomic neuropathy.

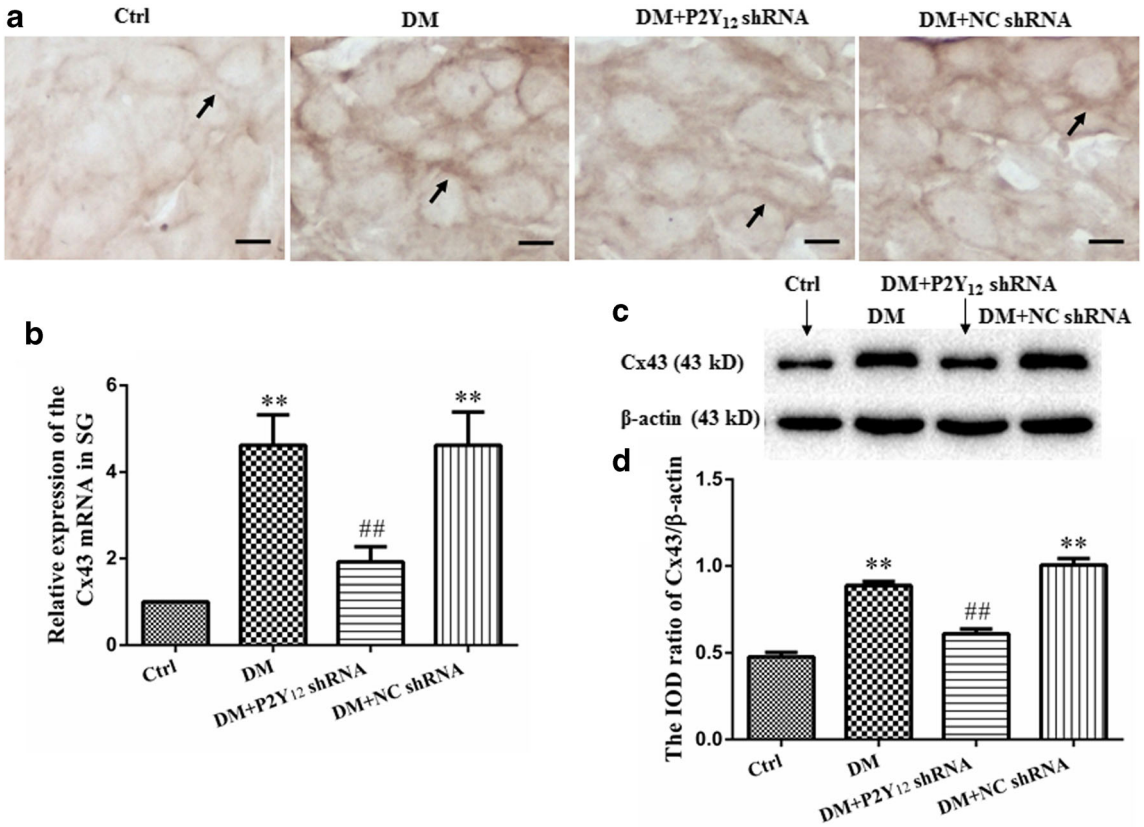

Fig. 7 The effects of $P2Y_{12}$ shRNA on the expression of Cx43 in SG of type 2 diabetic rats. **a** The expression of Cx43 was detected by immunohistochemistry. Scale bar, 20 μm. **b** The mRNA level of Cx43 was examined by real-time PCR. **c** The protein level of Cx43 was measured by Western blotting. **d** The bar histograms show the IOD ratio of Cx43 to β-actin in each group. Values are mean ± SEM from three independent experiments. $^{**}p < 0.01$ vs. Ctrl; $^{\#\#}p < 0.01$ vs. DM

The approach to introduce shRNA into rats used in this study might cause knockdown of the $P2Y_{12}$ receptor in all tissues and cells expressing it. Although the participation of other tissues/cells in the regulation of cardiovascular function cannot be excluded, several lines of evidence from this study strongly indicate a correlation between $P2Y_{12}$ activity in SGCs and cardiovascular autonomic neuropathy in diabetes. First, $P2Y_{12}$ receptor is expressed in microglial of the central nervous system [13]. It is also expressed in SGCs of SG [27]. Upregulation $P2Y_{12}$ receptor in the SGCs of superior cervical ganglia participates in the sympatho-excitatory reflex after myocardial ischemia [23]. Second, overexpression of $P2Y_{12}$ receptor in SG increased blood pressure, heart rate and cervical SND in non-diabetic rats whereas treatment of $P2Y_{12}$ shRNA could decrease the elevated blood pressure, heart rate and cervical SND occurring in diabetic rats. Third, our results of double-label immunofluorescence staining revealed that $P2Y_{12}$ receptor was coexpressed with GS (a marker of SGCs) but not colocalized with CGRP (expressed in neurons), indicating that $P2Y_{12}$ receptor was expressed in SGCs rather than neurons in SG. Thus, the $P2Y_{12}$ receptor in SGCs may be implicated in pathophysiological cardiovascular changes in diabetes.

MAPKs are a family of signaling molecules, transducing extracellular stimuli into intracellular responses in a wide variety of circumstances [46]. P38 MAPK is a member of MAPKs, and inflammation induces an increase in active p-p38 MAPK [47]. Recent studies have shown that $P2Y_{12}$ receptor can activate p38 MAPK signaling pathway [48]. Stimulation of $P2Y_{12}$ receptor by released ATP or the hydrolyzed products may enhance p38 MAPK activity, since intrathecal infusion of the $P2Y_{12}$ agonist 2-(methythio) adenosine 5′-diphosphate (2Me-SADP) into naive rats induced phosphorylation of p38 MAPK in spinal microglia and elevated pain behaviors [49, 50]. Both the pharmacological blockade by intrathecal administration of $P2Y_{12}$ antagonist and the antisense knockdown of $P2Y_{12}$ expression also suppressed not only the development of pain behaviors but also the phosphorylation of p38 MAPK in spinal microglia after partial sciatic nerve ligation (PSNL) or induced by 2Me-SADP [49, 50]. We found that phosphorylation of p38 MAPK in SG was significantly increased in type 2 diabetic rats and the activation of p38 MAPK in SG was remarkably inhibited in diabetic rats treated with $P2Y_{12}$ shRNA, further demonstrating the important role of $P2Y_{12}$ receptor in SG activation and subsequent inflammatory responses. There are communications between

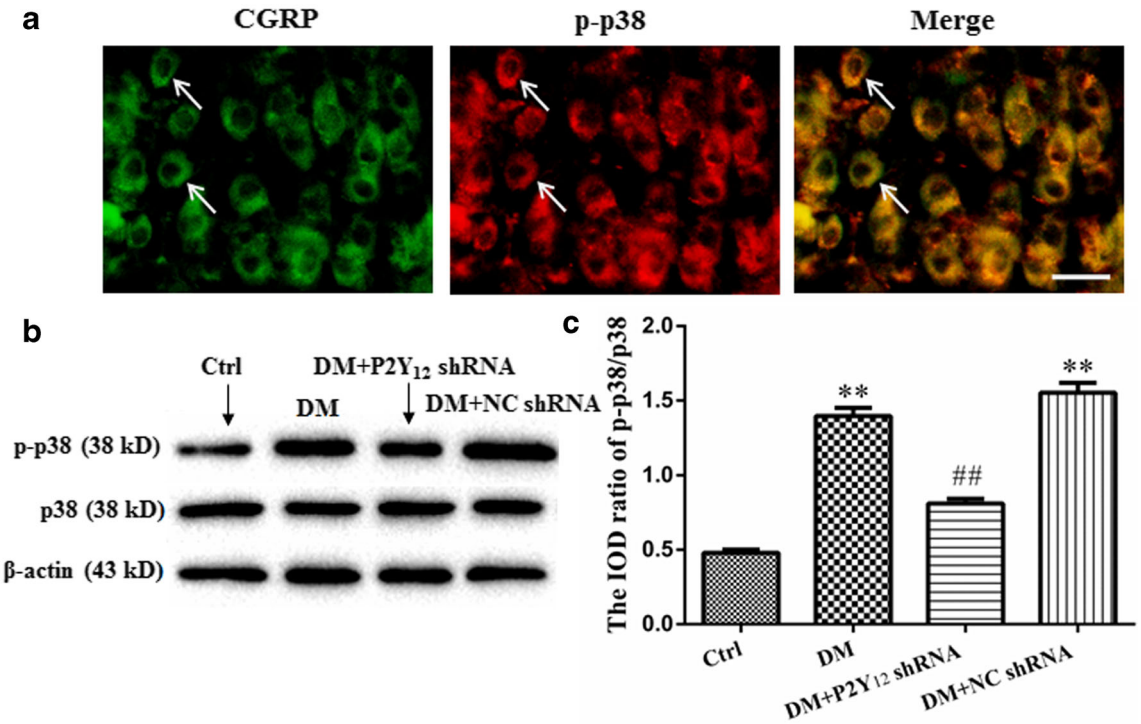

Fig. 8 The effects of $P2Y_{12}$ shRNA on the phosphorylation level of p38MAPK in SG of type 2 diabetic rats. **a** Double-label immunofluorescence staining of p-p38 MAPK and CGRP. The green signal represents CGRP staining with FITC, and the red signal indicates p-p38 MAPK staining with TRITC. Merged image denotes the p-p38 MAPK and CGRP double staining. Scale bar, 20 μm. **b** The expression levels of p38 MAPK and p-p38 MAPK were detected by Western blotting. **c** The bar histograms show the IOD ratio of p-p38 MAPK to p38 MAPK in each group. The values are mean ± SEM from three independent experiments. $^{**}p < 0.01$ vs. Ctrl; $^{\#\#}p < 0.01$ vs. DM

neurons and glial cells in the sympathetic ganglia [27] and activation of $P2Y_{12}$ receptor by ATP and ADP in DRG SGCs may mediate the neuron-to-glia communication [41, 51]. This study revealed that $P2Y_{12}$ and p38 MAPK appeared to present dominantly in SGCs and neurons, respectively, suggesting the communication between the two types of cells in SG. The observed activation of p38 MAPK in neurons could be due to enhanced release of pro-inflammatory molecules from SGCs following increased activity of $P2Y_{12}$ receptor under diabetic condition.

Type 2 diabetes is considered to be associated with chronic inflammatory responses. SGCs possess functions similar to those of astrocytes in the central nervous system; for example, they release pro-inflammatory cytokines such as IL-1β, IL-6, TNF-α, and monocyte chemoattractant protein-1 (MCP-1) and mediate the inflammatory response [27, 52]. The expression of these cytokines may be increased markedly under neurotoxic and inflammatory conditions [53]. In the process of injury and inflammation, the hyperactivity of neurons can lead to SGC activation, which in turn induces the proliferation of glial cells and increases the expression of certain regulatory proteins (e.g., glial fibrillary acidic protein and GS) and inflammatory mediators [54]. Our results showed that the expression of IL-1β and TNF-α at both mRNA and protein level in SGCs was upregulated in diabetic rats, suggesting that the hyperglycemic environment of diabetes could enhance the release of inflammatory factors. Furthermore, $P2Y_{12}$ shRNA significantly mitigated the upregulated expression of IL-1β and TNF-α due to diabetes, strengthening the notion that $P2Y_{12}$ receptor may regulate the expression of inflammatory factors in SGCs. Connexins (Cxs) are the structural subunits of both single membrane channels (also referred to as "hemichannels" or "connexons") in nonjunctional membranes and gap junction channels. Cx43 is the major Cxs expressed in SGCs and astrocytes [55]. Our results also revealed that the expression levels of Cx43 mRNA and protein in diabetic rats were increased. In addition, the hyperglycemic environment of diabetes may upregulate gap junction proteins, and thus enhances the interaction between SGCs and neurons, facilitating inflammatory responses. The gap junction may mediate the coupling of SGCs and directs the movement of the small molecule and metabolites between adjacent cells [56]. The abnormal interaction might aggravate the neuronal damage which contributes to the typical symptom of DCAN. We found that $P2Y_{12}$ shRNA significantly decreased the upregulated expression of Cx43 in SGCs of diabetic rats. Therefore, SGC activation in SG may also play an important role in the development of DCAN.

In conclusion, $P2Y_{12}$ shRNA treatment could suppress the elevated expression of $P2Y_{12}$ receptor and Cx43, inhibit p38 MAPK activation and the release of inflammatory cytokines in SG, improve the impaired sympathetic function, and

thereby alleviate cardiovascular autonomic neuropathy in diabetes. Thus, $P2Y_{12}$ receptor may be involved in the pathogenesis of DCAN and the $P2Y_{12}$ receptor may be exploited as a potential target for dealing with DCAN.

Acknowledgments This study was supported by grants from the National Natural Science Foundation of China (81560219, 31560276, 81570735, and 81200853), a grant from the young scientist training object of Jiangxi Province (20153BCB23030), and a grant from the Natural Science Foundation of Jiangxi Province (20171BAB205025).

Compliance with ethical standards

Conflicts of interest Jingjing Guo declares that she has no conflict of interest.
Xuan Sheng declares that she has no conflict of interest.
Yu Dan declares that she has no conflict of interest.
Yurong Xu declares that she has no conflict of interest.
Yuanruohan Zhang declares that he has no conflict of interest.
Huihong Ji declares that she has no conflict of interest.
Jiayue Wang declares that she has no conflict of interest.
Zixi Xu declares that she has no conflict of interest.
Hongyu Che declares that she has no conflict of interest.
Guodong Li declares that he has no conflict of interest.
Shangdong Liang declares that he has no conflict of interest.
Guilin Li declares that she has no conflict of interest.

Ethical approval The use of animals was reviewed and approved by the Animal Care and Use Committees of Nanchang University Medical Schools.

References

1. Li XQ, Zheng X, Chen M, Zhao MH (2017) Characteristics of diabetic nephropathy patients without diabetic retinopathy: a retrospective observational study. Medicine (Baltimore) 96:e6805
2. Ma RC, Chan JC (2013) Type 2 diabetes in East Asians: similarities and differences with populations in Europe and the United States. Ann N Y Acad Sci 1281:64–91
3. Rahelic D (2016) 7th edition of Idf diabetes atlas—call for immediate action. Lijec Vjesn 138:57–58
4. Jin J, Wang W, Zhu L, Gu T, Niu Q et al (2017) Cardiovascular autonomic neuropathy is an independent risk factor for left ventricular diastolic dysfunction in patients with type 2 diabetes. Biomed Res Int 2017:3270617
5. Tesfaye S, Boulton AJ, Dyck PJ, Freeman R, Horowitz M et al (2010) Diabetic neuropathies: update on definitions, diagnostic criteria, estimation of severity, and treatments. Diabetes Care 33: 2285–2293
6. Spallone V, Ziegler D, Freeman R, Bernardi L, Frontoni S, Pop-Busui R, Stevens M, Kempler P, Hilsted J, Tesfaye S, Low P, Valensi P, on behalf of The Toronto Consensus Panel on Diabetic Neuropathy (2011) Cardiovascular autonomic neuropathy in diabetes: clinical impact, assessment, diagnosis, and management. Diabetes Metab Res Rev 27:639–653
7. Pop-Busui R, Low PA, Waberski BH, Martin CL, Albers JW, Feldman EL, Sommer C, Cleary PA, Lachin JM, Herman WH, for the DCCT/EDIC Research Group (2009) Effects of prior intensive insulin therapy on cardiac autonomic nervous system function in type 1 diabetes mellitus: the Diabetes Control and Complications Trial/Epidemiology of Diabetes Interventions and Complications study (DCCT/EDIC). Circulation 119:2886–2893
8. Burnstock G (2007) Physiology and pathophysiology of purinergic neurotransmission. Physiol Rev 87:659–797
9. Qureshi IA, Mattick JS, Mehler MF (2010) Long non-coding RNAs in nervous system function and disease. Brain Res 1338: 20–35
10. Burnstock G, Krugel U, Abbracchio MP, Illes P (2011) Purinergic signalling: from normal behaviour to pathological brain function. Prog Neurobiol 95:229–274
11. Hollopeter G, Jantzen HM, Vincent D, Li G, England L, Ramakrishnan V, Yang RB, Nurden P, Nurden A, Julius D, Conley PB (2001) Identification of the platelet ADP receptor targeted by antithrombotic drugs. Nature 409:202–207
12. Gachet C (2012) P2Y(12) receptors in platelets and other hematopoietic and non-hematopoietic cells. Purinergic Signal 8:609–619
13. Sasaki Y, Hoshi M, Akazawa C, Nakamura Y, Tsuzuki H, Inoue K, Kohsaka S (2003) Selective expression of Gi/o-coupled ATP receptor P2Y12 in microglia in rat brain. Glia 44:242–250
14. Haynes SE, Hollopeter G, Yang G, Kurpius D, Dailey ME, Gan WB, Julius D (2006) The P2Y12 receptor regulates microglial activation by extracellular nucleotides. Nat Neurosci 9:1512–1519
15. Suadicani SO, Cherkas PS, Zuckerman J, Smith DN, Spray DC, Hanani M (2010) Bidirectional calcium signaling between satellite glial cells and neurons in cultured mouse trigeminal ganglia. Neuron Glia Biol 6:43–51
16. Yi Z, Xie L, Zhou C, Yuan H, Ouyang S et al (2017) P2Y12 receptor upregulation in satellite glial cells is involved in neuropathic pain induced by HIV glycoprotein 120 and 2′,3′-dideoxycytidine. Purinergic Signal. https://doi.org/10.1007/s11302-11017-19594-z
17. Tu G, Li G, Peng H, Hu J, Liu J, Kong F, Liu S, Gao Y, Xu C, Xu X, Qiu S, Fan B, Zhu Q, Yu S, Zheng C, Wu B, Peng L, Song M, Wu Q, Liang S (2013) P2X(7) inhibition in stellate ganglia prevents the increased sympathoexcitatory reflex via sensory-sympathetic coupling induced by myocardial ischemic injury. Brain Res Bull 96: 71–85
18. Burnstock G, Pelleg A (2015) Cardiac purinergic signalling in health and disease. Purinergic Signal 11:1–46
19. Wittfeldt A, Emanuelsson H, Brandrup-Wognsen G, van Giezen JJ, Jonasson J et al (2013) Ticagrelor enhances adenosine-induced coronary vasodilatory responses in humans. J Am Coll Cardiol 61: 723–727
20. Bell RM, Sivaraman V, Kunuthur SP, Cohen MV, Downey JM, Yellon DM (2015) Cardioprotective properties of the platelet P2Y12 receptor inhibitor, cangrelor: protective in diabetics and reliant upon the presence of blood. Cardiovasc Drugs Ther 29:415–418
21. Yang XM, Liu Y, Cui L, Yang X, Liu Y, Tandon N, Kambayashi J, Downey JM, Cohen MV (2013) Platelet P2Y12 blockers confer direct postconditioning-like protection in reperfused rabbit hearts. J Cardiovasc Pharmacol Ther 18:251–262
22. Jia T, Rao J, Zou L, Zhao S, Yi Z et al (2017) Nanoparticle-encapsulated curcumin inhibits diabetic neuropathic pain involving the P2Y12 receptor in the dorsal root ganglia. Front Neurosci 11: 755
23. Zou L, Gong Y, Zhao S, Yi Z, Han X, Wu B, Jia T, Li L, Yuan H, Shi L, Zhang C, Gao Y, Li G, Xu H, Liu H, Liang S, Liu S (2018) Downregulation of P2Y12 in the superior cervical ganglia alleviates abnormal sympathetic activity after myocardial ischemia. J Cell Physiol 233:3375–3383
24. Tu G, Zou L, Liu S, Wu B, Lv Q, Wang S, Xue Y, Zhang C, Yi Z, Zhang X, Li G, Liang S (2016) Long noncoding NONRATT021972 siRNA normalized abnormal sympathetic activity mediated by the upregulation of P2X7 receptor in superior cervical ganglia after myocardial ischemia. Purinergic Signal 12: 521–535

25. Pather N, Partab P, Singh B, Satyapal KS (2003) The sympathetic contributions to the cardiac plexus. Surg Radiol Anat 25:210–215
26. Fudim M, Boortz-Marx R, Ganesh A, Waldron NH, Qadri YJ, Patel CB, Milano CA, Sun AY, Mathew JP, Piccini JP (2017) Stellate ganglion blockade for the treatment of refractory ventricular arrhythmias: a systematic review and meta-analysis. J Cardiovasc Electrophysiol 28:1460–1467
27. Hanani M (2010) Satellite glial cells in sympathetic and parasympathetic ganglia: in search of function. Brain Res Rev 64:304–327
28. Costa FA, Moreira Neto FL (2015) Satellite glial cells in sensory ganglia: its role in pain. Rev Bras Anestesiol 65:73–81
29. Kobayashi K, Yamanaka H, Noguchi K (2013) Expression of ATP receptors in the rat dorsal root ganglion and spinal cord. Anat Sci Int 88:10–16
30. Horvath G, Goloncser F, Csolle C, Kiraly K, Ando RD et al (2014) Central P2Y12 receptor blockade alleviates inflammatory and neuropathic pain and cytokine production in rodents. Neurobiol Dis 70: 162–178
31. Katagiri A, Shinoda M, Honda K, Toyofuku A, Sessle BJ et al (2012) Satellite glial cell P2Y12 receptor in the trigeminal ganglion is involved in lingual neuropathic pain mechanisms in rats. Mol Pain 8:23
32. Feldman-Goriachnik R, Belzer V, Hanani M (2015) Systemic inflammation activates satellite glial cells in the mouse nodose ganglion and alters their functions. Glia 63:2121–2132. https://doi.org/10.1002/glia.22881
33. Rao S, Liu S, Zou L, Jia T, Zhao S, Wu B, Yi Z, Wang S, Xue Y, Gao Y, Xu C, Li G, Xu H, Zhang C, Liang S (2017) The effect of sinomenine in diabetic neuropathic pain mediated by the P2X3 receptor in dorsal root ganglia. Purinergic Signal 13:227–235
34. Liu S, Zou L, Xie J, Xie W, Wen S, Xie Q, Gao Y, Li G, Zhang C, Xu C, Xu H, Wu B, Lv Q, Zhang X, Wang S, Xue Y, Liang S (2016) LncRNA NONRATT021972 siRNA regulates neuropathic pain behaviors in type 2 diabetic rats through the P2X7 receptor in dorsal root ganglia. Mol Brain 9:44
35. Li G, Xu H, Zhu S, Xu W, Qin S, Liu S, Tu G, Peng H, Qiu S, Yu S, Zhu Q, Fan B, Zheng C, Li G, Liang S (2013) Effects of neferine on CCL5 and CCR5 expression in SCG of type 2 diabetic rats. Brain Res Bull 90:79–87
36. Wang M, Li S, Zhou X, Huang B, Zhou L, Li X, Meng G, Yuan S, Wang Y, Wang Z, Wang S, Yu L, Jiang H (2017) Increased inflammation promotes ventricular arrhythmia through aggravating left stellate ganglion remodeling in a canine ischemia model. Int J Cardiol 248:286–293
37. Lu Y, Wu Q, Liu LZ, Yu XJ, Liu JJ et al (2018) Pyridostigmine protects against cardiomyopathy associated with adipose tissue browning and improvement of vagal activity in high-fat diet rats. Biochim Biophys Acta 1864:1037–1050
38. Kenney MJ, Ganta CK, Fels RJ (2013) Disinhibition of RVLM neural circuits and regulation of sympathetic nerve discharge at peak hyperthermia. J Appl Physiol (1985) 115:1297–1303
39. Tiftikcioglu BI, Bilgin S, Duksal T, Kose S, Zorlu Y (2016) Autonomic neuropathy and endothelial dysfunction in patients with impaired glucose tolerance or type 2 diabetes mellitus. Medicine (Baltimore) 95:e3340
40. Erlinge D, Burnstock G (2008) P2 receptors in cardiovascular regulation and disease. Purinergic Signal 4:1–20
41. Magni G, Ceruti S (2013) P2Y purinergic receptors: new targets for analgesic and antimigraine drugs. Biochem Pharmacol 85:466–477
42. Burnstock G, Novak I (2013) Purinergic signalling and diabetes. Purinergic Signal 9:307–324
43. Wu B, Zhang C, Zou L, Ma Y, Huang K, Lv Q, Zhang X, Wang S, Xue Y, Yi Z, Jia T, Zhao S, Liu S, Xu H, Li G, Liang S (2016) LncRNA uc.48+ siRNA improved diabetic sympathetic neuropathy in type 2 diabetic rats mediated by P2X7 receptor in SCG. Auton Neurosci 197:14–18
44. Morel O, Kessler L, Ohlmann P, Bareiss P (2010) Diabetes and the platelet: toward new therapeutic paradigms for diabetic atherothrombosis. Atherosclerosis 212:367–376
45. Tarvainen MP, Laitinen TP, Lipponen JA, Cornforth DJ, Jelinek HF (2014) Cardiac autonomic dysfunction in type 2 diabetes - effect of hyperglycemia and disease duration. Front Endocrinol (Lausanne) 5:130
46. Jin SX, Zhuang ZY, Woolf CJ, Ji RR (2003) p38 mitogen-activated protein kinase is activated after a spinal nerve ligation in spinal cord microglia and dorsal root ganglion neurons and contributes to the generation of neuropathic pain. J Neurosci 23:4017–4022
47. Ji RR, Samad TA, Jin SX, Schmoll R, Woolf CJ (2002) p38 MAPK activation by NGF in primary sensory neurons after inflammation increases TRPV1 levels and maintains heat hyperalgesia. Neuron 36:57–68
48. Liu M, Yao M, Wang H, Xu L, Zheng Y, Huang B, Ni H, Xu S, Zhou X, Lian Q (2017) P2Y12 receptor-mediated activation of spinal microglia and p38MAPK pathway contribute to cancer-induced bone pain. J Pain Res 10:417–426
49. Kobayashi K, Yamanaka H, Fukuoka T, Dai Y, Obata K, Noguchi K (2008) P2Y12 receptor upregulation in activated microglia is a gateway of p38 signaling and neuropathic pain. J Neurosci 28: 2892–2902
50. Tatsumi E, Yamanaka H, Kobayashi K, Yagi H, Sakagami M, Noguchi K (2015) RhoA/ROCK pathway mediates p38 MAPK activation and morphological changes downstream of P2Y12/13 receptors in spinal microglia in neuropathic pain. Glia 63:216–228
51. Ceruti S, Fumagalli M, Villa G, Verderio C, Abbracchio MP (2008) Purinoceptor-mediated calcium signaling in primary neuron-glia trigeminal cultures. Cell Calcium 43:576–590
52. Hanani M (2005) Satellite glial cells in sensory ganglia: from form to function. Brain Res Brain Res Rev 48:457–476
53. Heinzmann S, McMahon SB (2011) New molecules for the treatment of pain. Curr Opin Support Palliat Care 5:111–115
54. Warwick RA, Hanani M (2013) The contribution of satellite glial cells to chemotherapy-induced neuropathic pain. Eur J Pain 17: 571–580
55. Spray DC, Hanani M (2017) Gap junctions, pannexins and pain. Neurosci Lett. https://doi.org/10.31016/j.neulet.32017.30506.30035
56. Lurtz MM, Louis CF (2007) Purinergic receptor-mediated regulation of lens connexin43. Invest Ophthalmol Vis Sci 48:4177–4186